TÉCNICO LISBOA

Extended abstract

Hardness modelling of porous copper bodies

Hugo Miguel Vicente Cardoso

hugo.vicente.cardoso@tecnico.ulisboa.pt

Instituto Superior Técnico, University of Lisbon

Abstract

Spherical powders are essential for additive manufacturing of metallic components. These processes require high powder flowability provided by particles with spherical shape. Also, powder made components are prone to develop residual porosity or can be developed with controlled porosity. Hardness testing is a rapid tool to access resistance to plastic flow of metallic materials. This resistance depends on component porosity.

This work proposes to model the hardness dependence on porosity using finite element experiments. It also proposes a method to develop spherical powders usable to produce model materials with controlled porosity. Pure copper and Brinell hardness testing were selected for the FEM experiments. Electrolytic dendritic copper powders were select for the liquid metal spheroidization process.

Spheroidization was carried out using a non-wettable graphite powder bed, using an in situ melting solidification process. Copper powders were heat treated in a primary vacuum furnace using a graphite powder bed and graphite dies. The analysed variables were temperature, holding time, copper/graphite mass ratio (CGR) and applied stress. Copper was separated from the mixture using a warm hydrochloric acid aqueous solution. The samples were characterized by SEM and EDS. The best spheroidization shape factor, 1.55±0.46, was achieved for copper powders processed at 1100ºC for 30 minutes, with low applied stress, in a mix with graphite KS4 and a CGR of 1:1.

FEM simulations were carried out to study the influence of porosity and load/indenter size ratio, F/D² ratio, on materials hardness. The GTN model was used to simulate a porous copper body. A direct linear relationship was observed between Brinell hardness and relative density. For copper, and for a void volume fraction (VVF) between 0 and 0.1, Brinell hardness simulation results can be expressed in a single equation, $BHN = 74{,}9 \cdot (F/D^2)_h^{-0{,}065} - 187{,}7 \cdot VVF \cdot (F/D^2)_h^{-0{,}215}$, where $(F/D^2)_h$ is the F/10D² dimensionless ratio and VVF the void volume fraction. Both densification, in the region beneath the indenter, and pile-up, at the periphery of the indentation, were observed. Pile-up was maximum for a 10 kgf/mm² F/D² ratio and 0% porosity.

Keywords: spherical powders; copper; graphite; finite element method; hardness; porosity

1. Introduction

Numerous industrial applications where metal powders play a key role require particles with increased flowability for processes such as additive manufacturing and metal powder injection where this parameter is critical. These powders also suit better the production of parts with controlled porosity than others, produced by water atomization or electrolysis, facilitating the production of model material for experimental validation of numerical simulation models.

The present work has two main goals: study and optimize a powder spheroidization process and introduce the study of hardness test simulations of porous metallic bodies using finite element method (FEM) experiments. This method capabilities can be useful to predict and explain experimental results in both dense and porous materials. Working with a model that successfully recreates reality also provides a reliable background for the development and improvement of constitutive equations for plastic flow in porous materials.

This work was structured into three different parts. The first part studies the production specifications and the parameters that influence this the production of spherical copper powders from dendritic powders using a melting/solidification process in a non wettable medium. The second part relates to the characterization of the spherical copper powders. The last part addresses the FEM study of the Brinell hardness test and the comparison between a pore-free and a porous copper material.

1.1. Spheroidization

The development of powder metallurgy, three-dimensional printing and metal injection moulding has led to a specific need for spherical powders, with fine particle size and smooth particle surface. The powder's shape and reduced size allow for a better compaction and therefore a higher and more homogeneous densification after sintering [1]. These benefits prompt increasing demand of spherical powders for part production.

Since the typical spherical powder production methods are rather cost demanding, a less expensive approach was tested based on melting/solidification method proposed in 2016 by Zhenzhi Cheng and co-authors [2]. This method rests on the principles of non-wettability. It consists in using a non wettable powder bed of graphite to separate liquid copper metallic particles and preventing the contact between them to avoid coalescence. By surrounding the copper particles with graphite platelets it is possible to create a localized region where the spheroidization will occur [1][3][4]. Between 1356.15 K and 2000 K, liquid copper's surface energy is over ten times that of graphite [5–7]. This difference will promote a non-wetting behaviour with contact angles $\theta > 150^{o}$ [8]. Thus copper droplets are expected to assume a spherical shape in order to reduce their surface energy [9].

1.2. Modelling

Indentation hardness tests, such as the Brinell hardness test, are extensively used in industry to assess plastic flow resistance and for quality control purposes. Hardness test modelling enables the verification and validation of constitutive models and the prediction of material properties without the need to fully

test them. In the case of porous materials, it would also be possible to evaluate the material's porosity fraction through hardness testing.

Detailed studies on contact mechanics involve mathematical complexities which can be solved with FEM. Literature reveals that FEM analysis is already used to predict and describe, with high confidence, the material's behaviour under compressive loads [10], with the possibility to test different porosity fractions.

The creation of a model that considers a porous metallic body requires the definition of constitutive equations for both the elastic and plastic regime. For isotropic materials, the elastic regime requires density, Young's modulus, and Poisson's ratio to create the material model. The plastic regime is created with plastic deformation models from uniaxial testing. However, since the model must account for porosity the latter model for plastic deformation is incomplete. One appropriate model is the Gurson-Tvergaard-Needleman (GTN) experimental model [11], [12].

2. Materials and Methods

2.1. Spheroidization

The copper powders spheroidization procedure was carried out with a graphite powder bed and dies, therefore creating a copper-graphite system. Two stainless steel cylindrical weights of different sizes were used to create pressure on the powder bed.

Two types of graphite, KS4 and PG10, and electrolytic copper powder were used in the spheroidization experiments with particle size of 3μm, 7μm and 31μm respectively. Analysis of particle size distribution of the original powders, both copper and graphite, was carried out on a Coulter LS230 Particle Size Analyzer.

Tailored amounts of copper and graphite powders were mixed in a turbula (Turbula T2C from Willy A. Bachofen) prior to the heat treatments. A quantity of approximately 0.26 g of powder mix was placed inside the mould in each experiment. Different copper-graphite mass ratios (CGR) were tested: 1:4; 1:2; 1:1 and 2:1.

Heat treatment of the powder mix were carried out in a high-density graphite resistance vacuum furnace (Thermal Technology's Model 1000). The primary vacuum level during the spheroidization procedure was of the order of 1 Pa. The copper-graphite system was first heated to 980ºC, and then subjected to two different temperatures, 1100ºC and 1200ºC, and two different time periods, 10 and 30 minutes. After the high temperature stage, the moulds cooled inside the furnace, and the powder mix was collected after unloading the furnace. This procedure was performed for two types of graphite, as shown on Table 1 and Table 2. Samples were labelled according to the graphite used, the applied stress, the spheroidization temperature and time and the mixture CGR.

Table 1 - Copper-Graphite PG10 powder mixture sample identification nomenclature.

			CGR	
T [°C]	t [min]	Applied stress	1:4	1:2
1100	30	0	PG 0:1100:30:1_4	PG 0:1100:30:1_2
		S	PG S:1100:30:1_4	PG S:1100:30:1_2
		B	PG B:1100:30:1_4	PG B:1100:30:1_2
	10	S	PG S:1100:10:1_4	-
1200	30	0	PG 0:1200:30:1_4	-
		S	PG S:1200:30:1_4	-
	10	0	PG 0:1200:10:1_4	-

Table 2 - Copper-Graphite KS4 powder mixture sample identification nomenclature.

			Copper-Graphite Ratio			
T [°C]	t [min]	Applied stress	1:4	1:2	1:1	2:1
1100	30	0	KS 0:1100:30:1_4	KS 0:1100:30:1_2	KS S:1100:30:1_1	-
		S	KS S:1100:30:1_4	KS S:1100:30:1_2	KS 0:1100:30:1_1	-
		B	KS B:1100:30:1_4	KS B:1100:30:1_2	KS B:1100:30:1_1	-
	10	S	KS S:1100:10:1_4	-	-	-
1200	30	0	KS 0:1200:30:1_4	KS 0:1200:30:1_2	KS 0:1200:30:1_1	KS 0:1200:30:2_1
		S	KS S:1200:30:1_4	-	-	-
	10	0	KS 0:1200:10:1_4	KS 0:1200:10:1_2	KS 0:1200:10:1_1	KS 0:1200:10:2_1
		S	-	KS S:1200:10:1_2	KS S:1200:10:1_1	KS S:1200:10:2_1

2.2. Separation

The separation media was produced by adding 0,1 ml of hydrochloric acid (37 wt% concentration) to 200 ml of distilled water, previously heated to approximately 90ºC. The resulting solution has an acid concentration of 0.006M, which corresponds to a pH of 2.22. The solution was kept at a constant temperature. After one hour, the copper powders were collected at the bottom of the vial, while graphite was concentrated at the top. The separation procedure was only carried out for the KS4 graphite samples with CGR's of 1:1 and 2:1.

Scanning electron microscopy (SEM) was used to verify and characterize the powder's morphology and to assess their size. The microscope used, HITACHI S2400, was operated with a voltage of 25 kV and a working distance, WD, of 15 mm. The samples were all loose powders. Energy dispersive X-ray spectroscopy analysis (EDS) was carried out to evaluate the specimens' composition, using a Bruker Nano XFlash detector.

The spheroidized powders shape factor and diameter were measured for 100 particles, selected on the SEM micrographs taken from each sample that underwent the separation process. Particle size was measured by averaging two perpendicular diameters from each particle while the roundness degree of

the particles in each sample, was provided by the ratio of the two perpendicular diameters, with ImageJ software.

2.3. Modelling

The FEM model developed in this work was a 2D axisymmetric local model representing a Brinell hardness test on a porous copper body sample, as represented in Figure 1-a).

A preliminary study on the part's mesh and partition was carried out to understand the influence of the element's size and number on the simulation outputs. The final simulation model has a mesh composed of 42643 CAX4R quadrangular elements, as depicted in Figure 1-b). The boundary conditions applied to the model are shown in Figure 1-c). The porous copper material was created based on the GTN experimental model.

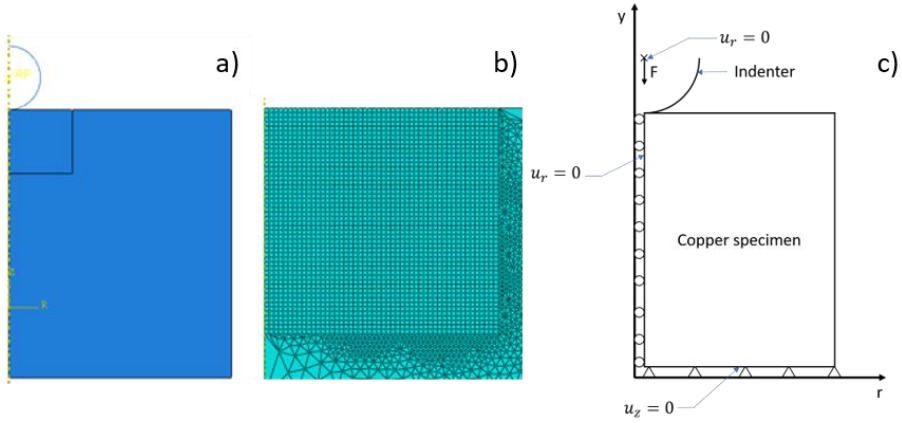

Figure 1 – a) Simulation model configuration of the assembly for the Brinell hardness test; b) Mesh used in the final simulations; c) Boundary conditions applied to both indenter and body.

Two conditions were studied in the model: applied loads and load/indenter size ratio (F/D^2).

The chosen loads for the first condition were: 1500, 1000 and 500 kgf, with one diameter indenter (10mm) and a relative density (porosity) that varies from 1 to 0.9 with 0.01 increments.

For the second condition, two F/D^2 ratios were selected: 10 and 5 kgf/mm²; three indenter diameters were used: 2.5, 5 and 10 mm; with three relative densities: 1, 0.95 and 0.9, and the load resulted from the F/D^2 ratio.

Five valuable output variables were identified: Von Mises stress (S), which assesses the stress applied on the body; equivalent plastic strain (EPS), that provides information on the body's deformation; contact pressure (CP), as endured by the body; void volume fraction (VVF) and void volume fraction growth (VVFG), which relate to the void amount and closure.

3. Results and Discussion

3.1. Spheroidization & separation processes

Copper particles were submitted to a spheroidization process on a graphite powder bed, under different processing parameters. Alterations on the previously dendritic particles were observed. Figure 2 shows

the morphology and size of the particles after both the spheroidization and separation processes. After the separation process, all the samples were observed on the SEM, and 100 particles per sample were measured. Small particles show a morphology that resembles a sphere, whereas bigger particles assumed an elongated shape due to powder coalescence.

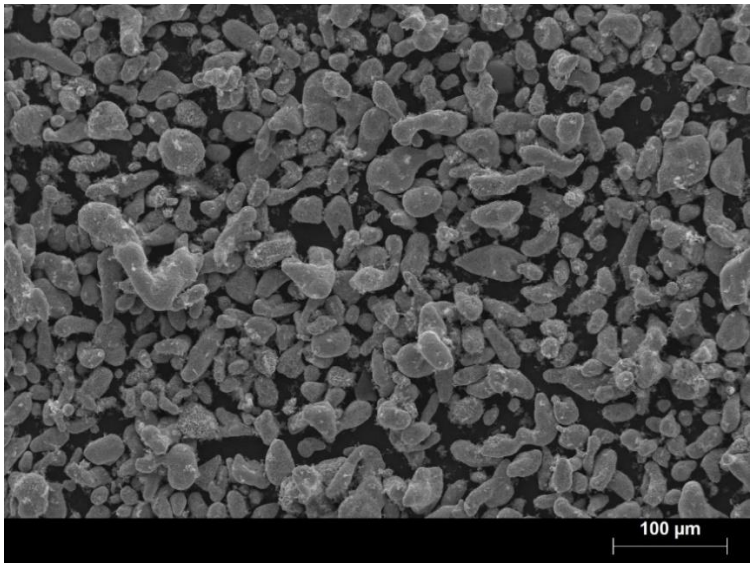

Figure 2 - SEM micrograph of sample KS B:1100:30:1_1 after powder separation. The bigger particles present an elongated shape whereas the smaller ones have more spherical morphologies.

Due to a high standard deviation, it is not possible to conclude the influence of each parameter on the spheroidization process.

The graphite-copper separation process is effective but induces changes in the previously spheroidized particles, as seen in Figure 3. After the separation procedure, some samples exhibited particles with cubes on their surfaces. No similar results were found in literature, thus further word on this topic is suggested to understand this occurrence. Since the primary purpose of this work's section was to spheroidize the copper particles, any morphology modification after this process is not desirable, hence an alternative separation method should be studied.

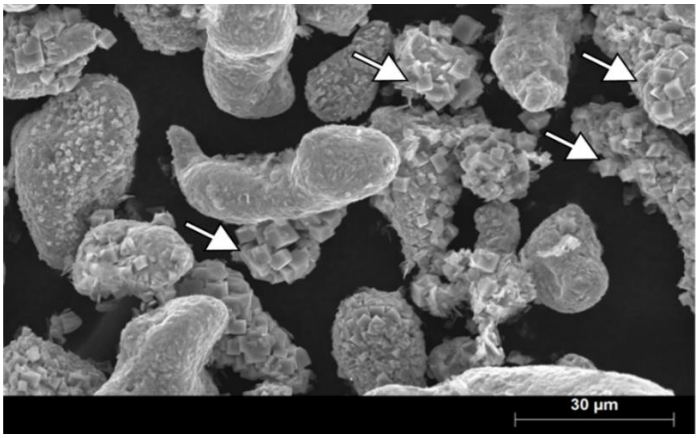

Figure 3 – Copper particles after separation, where corrosion effects are visible (identified with arrows).

3.2. FEM Simulations

Through this study it was verified that the BHN decreases linearly with relative density for all tested loads. Equations (1) to (3) are proposed to describe the BHN variation with relative density (RD).

$$BHN_{500} = 199.16 \cdot RD - 127.56 \qquad R^2 = 0.9798 \qquad (1)$$

$$BHN_{1000} = 189.05 \cdot RD - 114.26 \qquad R^2 = 0.9871 \qquad (2)$$

$$BHN_{1500} = 180.16 \cdot RD - 103.22 \qquad R^2 = 0.9995 \qquad (3)$$

A relationship between BHN and VVF, for any applied load, is proposed in equation (4):

$$BHN = 74.9 \cdot (F/D^2)_h^{-0.065} - 187.7 \cdot VVF \cdot (F/D^2)_h^{-0.215} \qquad R^2 = 0.9998 \qquad (4)$$

BHNs are corrected taking in account the F/D² ratio used. Considering that 10 represents a recommended F/D² ratio for copper and copper alloys a dimensionless homologous ratio, $(F/D^2)_h$, is defined as $(F/D^2)_h = F/(10 \cdot D^2)$. Figure 4, represents $BHN_h = BHN \cdot (F/D^2)_h^{0.065}$ as a function of the homologous volume void fraction $VVF_h = VVF \cdot (F/D^2)_h^{-0.15}$.

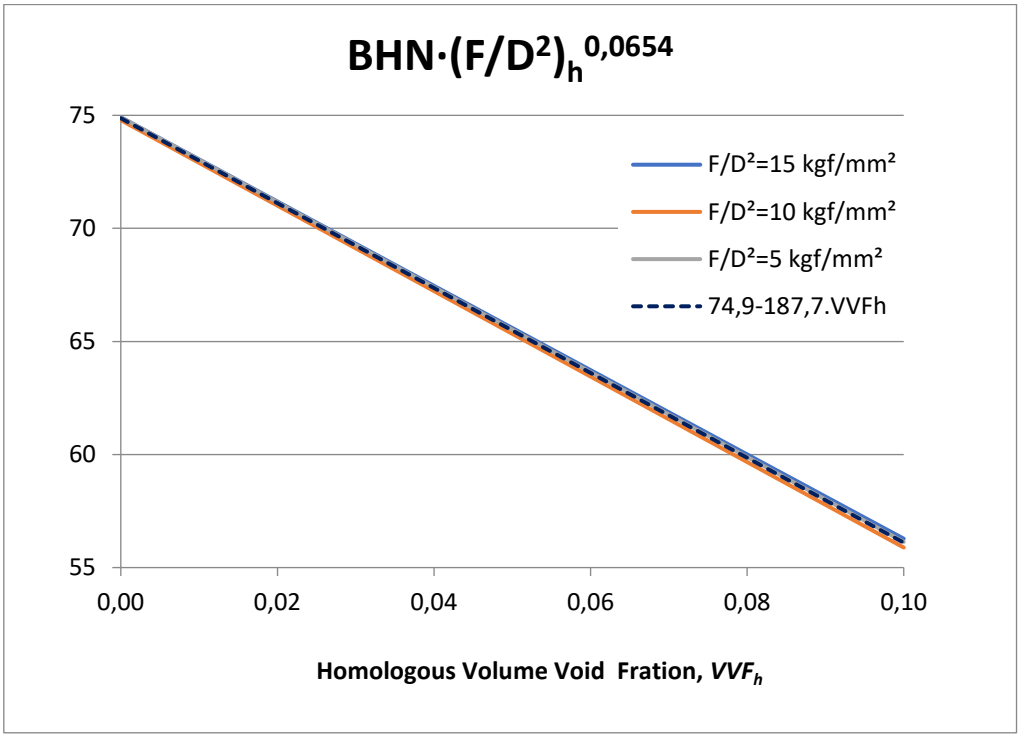

Figure 4 - Brinell Hardness simulation results for all load conditions. D=10mm.

The Von Mises Stress, The Equivalent Plastic Strain, the Volume Void Fraction, VVF, and the Volume Void Fraction Growth all present a parabolic dependence with relative density.

The Von Mises Stress decreases with decreasing relative density, since for the same volume there is less material to support the applied load.

The EPS maintains the same trend with relative density for all the applied loads. Higher loads induce higher values of EPS. Lower applied loads exhibit higher differences between 0 and 10% porosity.

For increasing porosity, with a higher applied load, VVF and VVFG present the lowest value, since there is more compaction due to higher plastic deformation.
For a 10 kgf/mm² F/D^2 ratio, the Von Mises stress at the end of the indentation step decreases when the relative density decreases, since there is less material to support the applied load. When the indenter size increases so does the Von Mises stress at the end of the indentation step. This is more preponderant for low porosity bodies. At the end of the removal step, the Von Mises stress decreases when relative density decreases. For a 5 kgf/mm² F/D^2 ratio, irregular variations are observed for a relative density of 0.9. No trend was observed for this value of F/D^2 when relative density decreased. This suggests that the model has application limits for lower applied loads at high porosity contents (10%).

At a F/D^2 ratio of 10 kgf/mm², the indenter's size has little influence on the BHN. It is observed that for 0% and 5% porosity there is a difference of 10 BHN between the two tested F/D^2 ratios. Under 5kgf/mm² and for 10% porosity the model shows low data consistency, thus suggesting that the GTN model has limitation for these conditions, as already mentioned.

Only pile-up effects were observed, for all the simulations. It has more influence in the BHN measurement for less porous materials, since for high porosity bodies (10% porosity) the pile-up effect is compensated by the void compaction during indentation.

4. Conclusion

4.1. Powder spheroidization

This work studies the influence of temperature, copper-graphite ratio (CGR), graphite powder size, applied stress and time on powder spheroidization.

Graphite powder size influence on spheroidization could not be assessed because not enough significant samples could be retrieved from the separation process.

The particle's shape of all the observed samples changed after the spheroidization process. Due to a high standard deviation, it is not possible to conclude the influence of each parameter on the spheroidization process.

Separation of copper and graphite powders was not feasible using only water as suspension medium and sonication. A hydrochloric aqueous solution was instead tested as a separation medium. This method effectively separates the two powders, but also modifies the particles morphology, because copper is corroded in the presence of chlorine ions.

Some samples exhibited particles with cubes on their surfaces after the separation procedure. No similar results were found in literature, thus further word on this topic is suggested to understand this occurrence.

The estimated shape factor for the initial dendritic powder was 2.67±0.54. A best shape factor of 1.55±0.46 is suggested for test carried out at 1100ºC for 30 minutes, under low applied stress with graphite KS4.

4.2. Simulations

Hardness test of porous copper bodies was simulated using a FEM approach. The Gurson-Tvergaard-Needleman (GTN) material model was used to simulate the porous body. The GTN and the Johnson-Cook models were matched against each other, and a good correlation was found for a full dense material. Quadrangular elements were chosen for the body mesh since those were found to adapt more easily to the body deformation that triangular elements.

The influence of porosity and the load/indenter's size ratio, F/D², on Brinell hardness number, BHN, was studied. BHN decreases linearly with relative density for all tested loads. Equations (1) to (3) are proposed to describe the BHN variation with relative density. Equation (4), $BHN = 74.9 \cdot (F/D^2)_h^{-0.065} - 187.7 \cdot VVF \cdot (F/D^2)_h^{-0.215}$, is proposed to describe the variation of BHN with VVF, for any given F/D² ratio.

The Von Mises Stress, The Equivalent Plastic Strain, the Volume Void Fraction, VVF, and the Volume Void Fraction Growth all present a parabolic dependence with relative density.

Von Mises stress decreases with decreasing relative density, since for the same volume there is less material to support the applied load. The equivalent plastic strain, EPS, maintains the same trend with relative density for all the applied loads. Higher loads induce higher values of EPS.

For increasing porosity, the volume void fraction, VVF, and the volume void fraction growth, VVFG, present the lowest value for a higher applied load, since there is more compaction due to higher plastic deformation.

Two F/D² ratios, 10 kgf/mm² and 5kgf/mm², were used to study the influence of this parameter and of the indenter size on BHN. For a F/D² ratio of 10 kgf/mm², the indenter's size has little influence on BHN. For 0% and 5% porosity, the difference between the two tested F/D² ratios is approximately 7.8 BHN (11.4%). For 5kgf/mm² and 10% porosity the model shows low data consistency, suggesting that the developed model has limitation for these conditions.

The pile-up, up flow of material around the indentation periphery, is present as a result of the FEM experiments. Results show that pile-up effect is more significant for low porosity samples. For higher porosities, the void compaction compensates this effect. Higher F/D² ratios increase the pile-up height.

The created model provided more consistent results for simulations with both high diameters and F/D² ratios for all the tested variables.

References

[1] C. Lei, H. Huang, Y. Huang, Z. Cheng, S. Tang, and Y. Du, “In-situ de-wetting assisted fabrication of spherical Cu-Sn alloy powder via the reduction of mixture metallic oxides,” *Powder Technol.*, vol. 301, pp. 356–359, 2016.

[2] Z. Cheng, C. Lei, H. Huang, S. Tang, and Y. Du, “The formation of ultrafine spherical metal powders using a low wettability strategy of solid-liquid interface,” *Mater. Des.*, vol. 97, pp. 324–330, 2016.

[3] C. Lei, H. Huang, Z. Cheng, S. Tang, and Y. Du, “Mono-disperse spherical Cu-Zn powder fabricated via the low wettability of liquid/solid interface,” *Appl. Surf. Sci.*, vol. 357, pp. 167–171, 2015.

[4] C. Lei, H. Huang, Z. Cheng, S. Tang, and Y. Du, “Fabrication of spherical Fe-based magnetic powders via the in situ de-wetting of the liquid-solid interface,” *RSC Adv.*, vol. 6, no. 5, pp. 3428–3432, 2016.

[5] I. Egry, E. Ricci, R. Novakovic, and S. Ozawa, “Surface tension of liquid metals and alloys-Recent developments,” *Adv. Colloid Interface Sci.*, vol. 159, no. 2, pp. 198–212, 2010.

[6] B. J. Keene, “Review of data for the surface tension of pure metals,” *Int. Mater. Rev.*, vol. 38, no. 4, pp. 157–192, 1993.

[7] P. D. Ownby and J. Liu, “Surface energy of liquid copper and single-crystal sapphire and the wetting behavior of copper on sapphire,” *J. Adhes. Sci. Technol.*, vol. 2, no. 1, pp. 255–269, 1988.

[8] D. A. Mortimer and M. Nicholas, “The wetting of carbon by copper and copper alloys,” *J. Mater. Sci.*, vol. 5, no. 2, pp. 149–155, 1970.

[9] P. Atkins and J. Paula, *Physical chemistry*. 2006.

[10] M. Sabzevari, R. J. Teymoori, and S. A. Sajjadi, “FE modeling of the compressive behavior of porous copper-matrix nanocomposites,” *Mater. Des.*, vol. 86, pp. 178–183, 2015.

[11] A. L. Gurson, “Continuum Theory of Ductile Rupture by Void Nucleation and Growth: Part I—Yield Criteria and Flow Rules for Porous Ductile Media,” *J. Eng. Mater. Technol.*, vol. 99, no. 1, pp. 2–15, 1977.

[12] V. Tvergaard, “Influence of voids on shear band instabilities under plane strain conditions,” *Int. J. Fract.*, vol. 17, no. 4, pp. 389–407, 1981.